Reduction of Artifacts in Computer Simulation of Breast Cooper's Ligaments

David D. Pokrajac[a], Adam Kuperavage[b], Andrew D.A. Maidment[c], Predrag R. Bakic[c]

[a]Dept. of Computer & Information Sciences, Delaware State University, Dover DE USA 19901
[b]Dept. of Public and Allied Health Sciences, Delaware State University, Dover DE USA 19901
[c]Dept. of Radiology, University of Pennsylvania, Philadelphia, PA USA 19104

ABSTRACT

Anthropomorphic software breast phantoms have been introduced as a tool for quantitative validation of breast imaging systems. Efficacy of the validation results depends on the realism of phantom images. The recursive partitioning algorithm based upon the octree simulation has been demonstrated as versatile and capable of efficiently generating large number of phantoms to support virtual clinical trials of breast imaging.

Previously, we have observed specific artifacts, (here labeled "dents") on the boundaries of simulated Cooper's ligaments. In this work, we have demonstrated that these "dents" result from the approximate determination of the closest simulated ligament to an examined subvolume (i.e., octree node) of the phantom. We propose a modification of the algorithm that determines the closest ligament by considering a pre-specified number of neighboring ligaments selected based upon the functions that govern the shape of ligaments simulated in the subvolume.

We have qualitatively and quantitatively demonstrated that the modified algorithm can lead to elimination or reduction of dent artifacts in software phantoms. In a proof-of concept example, we simulated a 450 ml phantom with 333 compartments at 100 micrometer resolution. After the proposed modification, we corrected 148,105 dents, with an average size of 5.27 voxels (5.27nl). We have also qualitatively analyzed the corresponding improvement in the appearance of simulated mammographic images. The proposed algorithm leads to reduction of linear and star-like artifacts in simulated phantom projections, which can be attributed to dents. Analysis of a larger number of phantoms is ongoing.

Keywords: Digital mammography, anthropomorphic breast phantoms, Cooper's ligaments, virtual clinical trials, computational geometry.

1. INTRODUCTION

Our recursive partitioning algorithm[1-6] provides an efficient method for fast simulation[7] of software breast phantoms, thus opening venues for virtual clinical trials[8] and other studies requiring a large number of simulated breasts, or breast images, with specified characteristics. The algorithm contains mechanisms to control thickness of Cooper's ligaments thus providing for realistic simulation of tissue. However, it has been observed that the simulation method can result in indentation artifacts[1], so called "dents", on the boundary of simulated Cooper's ligaments. These artifacts may affect the realism of obtained results.

Our purpose is to improve the quality of our recursive partitioning based breast phantom simulations by reducing these artifacts. The goal is to determine what causes the dents and to propose an algorithm modification that may improve the smoothness of simulated ligament surfaces. This way, we can reduce the dents in simulated phantoms. We provide qualitative and quantitative measures that indicate that the proposed changes in the simulation algorithm can lead to better quality of the produced phantoms and resulting simulated images.

Medical Imaging 2016: Physics of Medical Imaging, edited by Despina Kontos, Thomas G. Flohr, Joseph Y. Lo,
Proc. of SPIE Vol. 9783, 97832Q · © 2016 SPIE · CCC code: 1605-7422/16/$18 · doi: 10.1117/12.2217160

2. METHODS

2.1 Phenomenology of Dents

A recursive partitioning based simulation algorithm[1] utilizes an approximate method to determine the Cooper's ligament closest to cubic subvolumes of a simulated breast. Here we demonstrate that the application of this technique may lead to "dent"-like artifacts at the ligament borders.

The recursive algorithm[1] simulates 3D breast structures as generalized Voronoi regions[9]. This paradigm utilizes quadratic functions (referred to as shape functions):

$$f_i(\mathbf{x}) = \frac{1}{2}(\mathbf{x}-\mathbf{s}_i)^T \Sigma_i^{-1}(\mathbf{x}-\mathbf{s}_i) - \log q_i - \frac{1}{2}\log\det\left(\Sigma_i^{-1}\right),\ i=1,\ldots,\mathrm{K}, \quad (1)$$

to specify adipose and glandular compartments and Cooper's ligaments. A necessary condition for a point **x** to belong to a compartment C_i is:

$$f_i(\mathbf{x}) < f_j(\mathbf{x}),\ j \neq i. \quad (2)$$

If compartments C_i and C_j are adjacent, they are bounded with a ligament $L_{i,j}$. The ligament has a nominal thickness $2D$ (where D is a simulation parameter), and consists of points at a distance from a median surface $F_{i,j}(\mathbf{x})=0$ smaller than or equal to D, where $F_{i,j}(\mathbf{x}) = f_i(\mathbf{x}) - f_j(\mathbf{x})$. Consider a compartment C_i bounded by compartments $C_{j1},\ldots, C_{jM}$. A point $\mathbf{x} \in C_i \cup L_{i,j1} \ldots \cup L_{i,jM}$ is closest to a ligament $L_{i,j}$ if:

$$j = argmin_{j\in\{j1,\ldots,jM\}} d(\mathbf{x}, F_{i,j}=0), \quad (3)$$

where d denotes a Euclidean distance between a point and a surface $F_{i,j}=0$.

The algorithm[1] assigns points belonging to particular compartments and ligaments as follows. It starts from a rectangular region containing the breast outline and proceeds with recursive partitioning (into 8 sub-volumes) until a subvolume contains only one material (e.g., adipose) or until the minimal subvolume size (equal to the voxel size) has been achieved. To determine compartments/ligaments, the algorithm uses the following approximate approach: For each subvolume **B**, the algorithm evaluates the minimal and maximal values of shape functions associated to subvolume **B** (see Fig. 1). Let i and j be indices of shape functions that have the two smallest minima in **B** such that:

$$max_{\mathbf{x}\in B} f_i(\mathbf{x}) < min_{\mathbf{x}\in B} f_j(\mathbf{x}) \quad (4a)$$

and

$$min_{\mathbf{x}\in B} f_j(\mathbf{x}) \leq min_{k,k\neq i,j} min_{\mathbf{x}\in B} f_k(\mathbf{x}). \quad (4b)$$

The algorithm considers the subvolume **B** closest to ligament $L_{i,j}$ and base the further processing of the subvolume on calculating the minimal and maximal Euclidean distance $d_{i,j} \equiv min_{\mathbf{x}\in\mathbf{B}}(\mathbf{x}, F_{i,j}=0), D_{i,j} \equiv max_{\mathbf{x}\in\mathbf{B}}(\mathbf{x}, F_{i,j}=0)$ from **B** to the surface $F_{i,j}(\mathbf{x})=0$. Thus, the subvolume is assigned to a compartment C_i and not split if:

$$d_{i,j} > D. \quad (5a)$$

The subvolume is assigned to a ligament $L_{i,j}$ and is not split if:

$$D_{i,j} \leq D. \quad (5b)$$

Otherwise, the subvolume is on the boundary of ligament $L_{i,j}$, and is split into 8 subvolumes (unless it has reached the voxel size) and the following condition holds:

$$d_{i,j} \leq D, D_{i,j} > D. \quad (5c)$$

Note that condition, Eq. (4a), usually holds when a subvolume size is relatively small, hence minima and maxima of shape functions in a subvolume are approximately equal. Therefore for each point **x** in a subvolume approximately holds:

$$|F_{i,j}(\mathbf{x})| < |F_{i,k}(\mathbf{x})|,\ k \neq j, \quad (6)$$

i.e.,

$$j = argmin_k |F_{i,k}(\mathbf{x})|, \mathbf{x} \in \mathbf{B}. \quad (7)$$

Note, however, that the Euclidean and Mahalanobis[10] metrics are not equivalent, hence conditions Eq. (3) and Eq. (7) are not identical. Hence, the algorithm[1] may incorrectly detect the closest ligament to the subvolume **B**, see Fig. 2. Let a ligament $L_{ij'}$ be closest to a subvolume **B** while the algorithm pinpoints L_{ij} as the closest ligament (see Fig. 1). It is possible that $min_{\mathbf{x}\in\mathbf{B}}(\mathbf{x}, F_{i,j'}=0) \leq D$ but $min_{\mathbf{x}\in\mathbf{B}}(\mathbf{x}, F_{i,j}=0) > D$. As a consequence, the subvolume **B** that partially or completely belongs to a ligament $L_{i,j'}$ may be incorrectly assigned to a compartment, and thus, visible artifacts, ("dents") may appear on the ligament boundary.

Fig. 3. Illustrates the appearance of "dents" in a detail of a one slice of a simulated software breast phantom with 100μm linear voxel size. Fig. 4 shows color-coded sizes of subvolumes during recursive partitioning and indicates that the "dents" correspond to subvolumes of relatively small size (2—4 times the voxel size) that were incorrectly assigned to a compartmental tissue. Such subvolumes are frequently located in the vicinity of adjacent ligaments other than the ligament they should belong to; this supports the hypothesis that the dents are result of incorrect assignment of subvolumes to the nearest ligament.

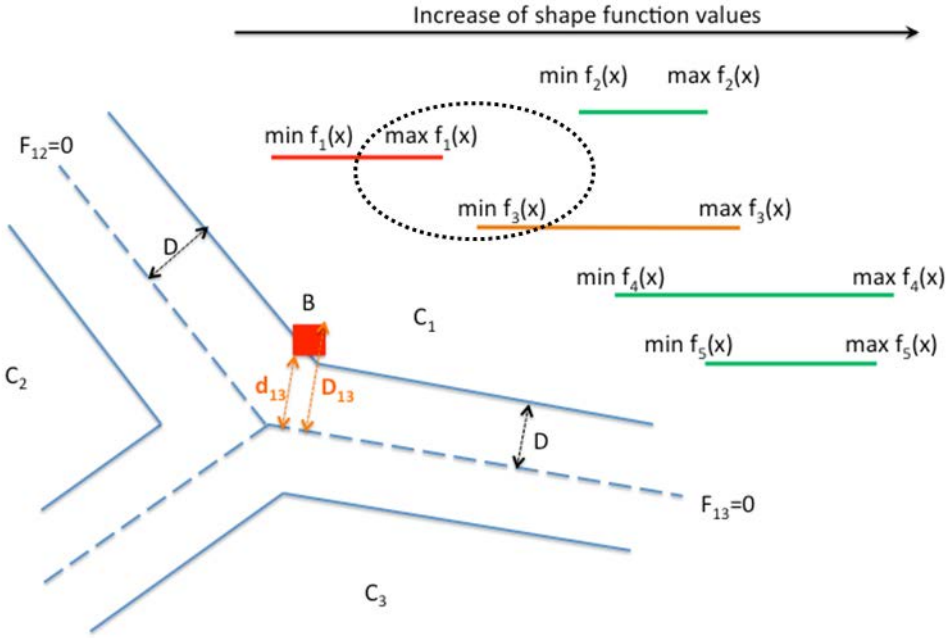

Figure 1. Illustration of the old algorithm[1] for simulating Cooper's ligaments. The maximal value of shape function f_1 in subvolume B is smaller than the minima of any other shape function. Shape function f_3 has the second smallest minimum of all the shape functions. The algorithm considers subvolume B closest to the ligament $L_{1,3}$, and thus calculates the distance of B from the surface $F_{1,3}(\mathbf{x})=0$, and assigns B to compartment C_1. (Note that the closest ligament to B is actually $L_{1,2}$ and that B intersects with $L_{1,2}$.)

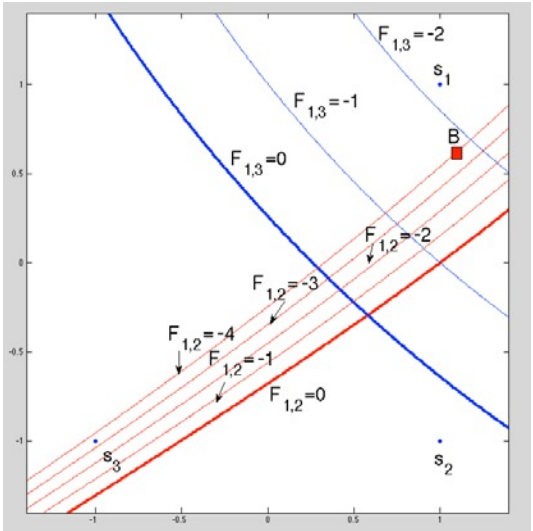

Figure 2. A case when the old algorithm[1] fails to identify the closest ligament to a subvolume B. Since $|F_{1,3}(\mathbf{x})|, \mathbf{x} \in \mathbf{B} < 2$ and $|F_{1,2}(\mathbf{x})|, \mathbf{x} \in \mathbf{B} > 3$, the algorithm determines ligament $L_{1,3}$ as closest to **B**. In fact, the Euclidean distance of **B** to the surface $F_{1,2}(\mathbf{x}) = 0$ is smaller than to $F_{1,3}(\mathbf{x}) = 0$ and hence **B** is closer to ligament $L_{1,2}$. Here, $\mathbf{s}_1$, $\mathbf{s}_2$ and $\mathbf{s}_3$ are parameters of shape functions, Eq. (1).

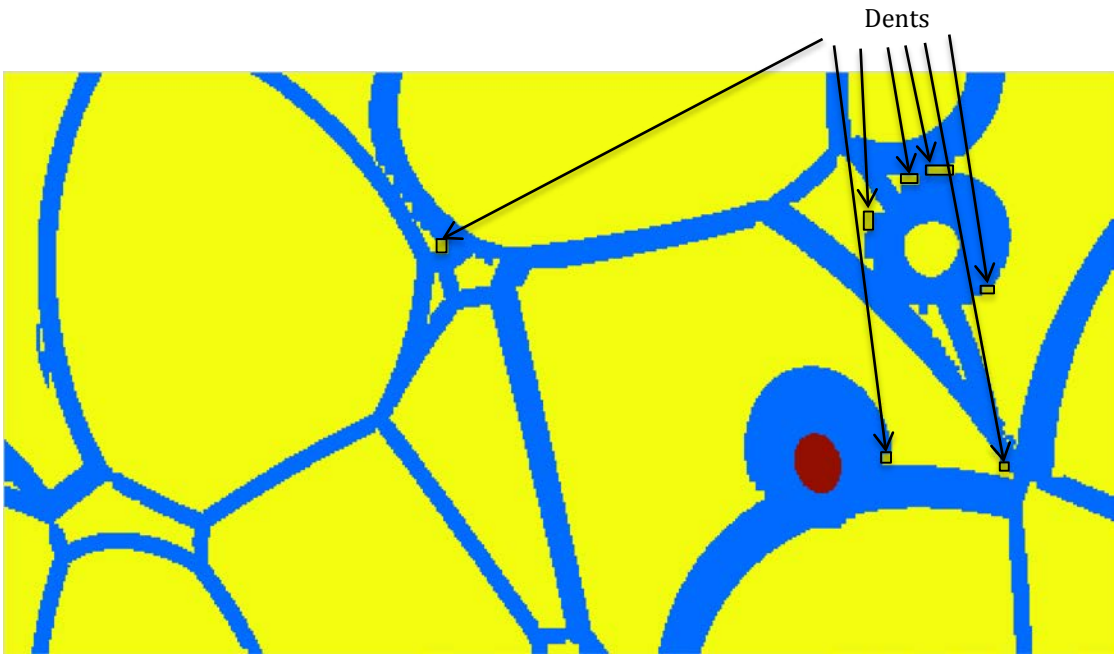

Figure 3. "Dents" visible on a detail of one slice of a simulated software breast phantom with 100μm linear voxel size.

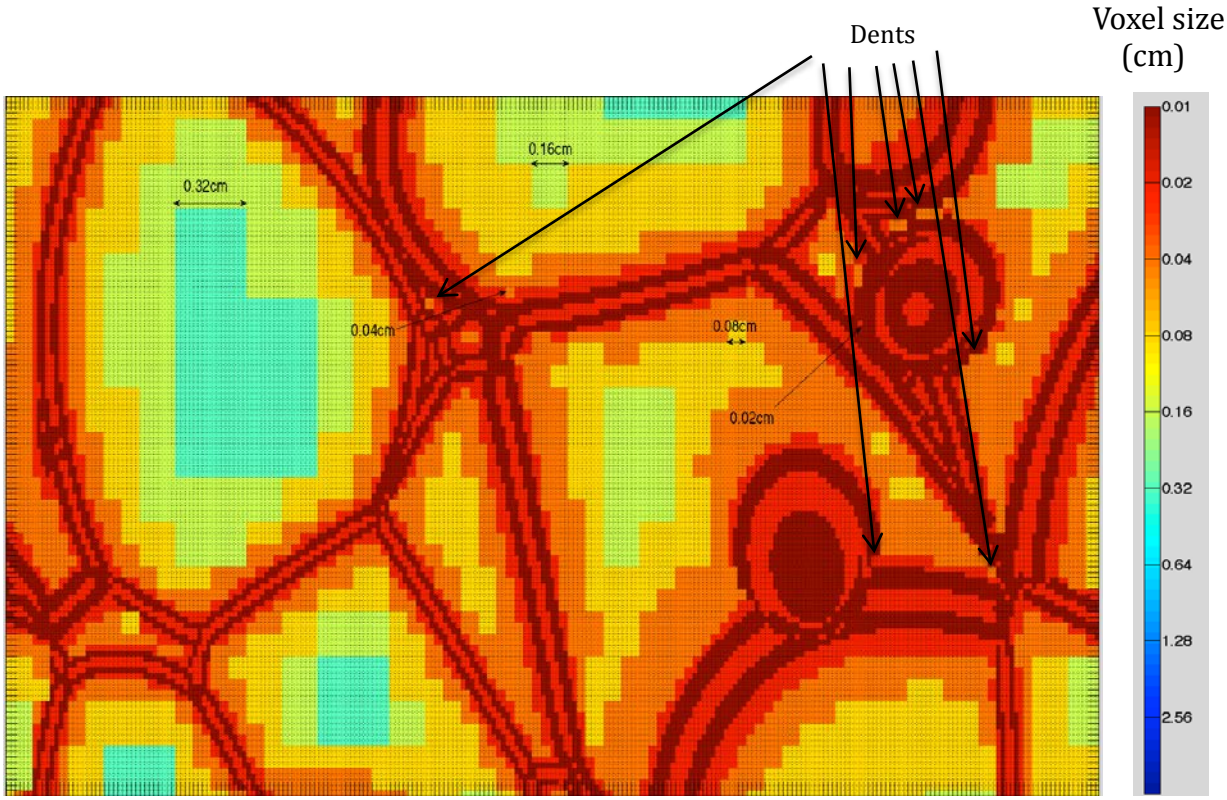

Figure 4. Color-coded subvolume sizes during recursive partitioning.

2.2 Proposed Algorithm

The proposed modification of the recursive partitioning simulation algorithm is aimed to improve handling of subvolumes containing ligaments and compartmental tissues in order to reduce "dents" on the ligament boundaries. Our idea is to keep *p* candidates for the closest ligament to a subvolume and to calculate Euclidean distance.

The algorithm performs as follows when conditions Eq. (4a, 4b) are satisfied. We determine $p>1$ shape functions such that:

$$max_{\mathbf{x}\in B} f_i(\mathbf{x}) < min_{\mathbf{x}\in B} f_{j1}(\mathbf{x}) \le min_{\mathbf{x}\in B} f_{j2}(\mathbf{x}) \le \cdots \le min_{\mathbf{x}\in B} f_{jp}(\mathbf{x}) \le min_{k\notin\{i,j1,\ldots,jp\}} min_{\mathbf{x}\in B} f_k(\mathbf{x}) \quad (8)$$

and compute minimal and maximal Euclidean distances $d_{i,j_1}, \ldots d_{i,j_p}$ and $D_{i,j_1}, \ldots D_{i,j_p}$ to the median surfaces $F_{i,j_1} = 0, \ldots, F_{i,j_p} = 0$ (see Fig. 5 for an example). Based on a comparison between the distances to the desired half-thickness of a ligament *D*, we distinguish whether a subvolume **B** belongs to a compartment, a boundary of one or several ligaments, or is completely contained within a ligament. Similarly, we decide whether the subvolume **B** need be subsequently split in the next recursive partitioning round. A subvolume **B** belongs to a compartment *i* and is not further split if:

$$d_{i,j_1}, \ldots d_{i,j_p} > D. \quad (9a)$$

The subvolume **B** is in the intersection of *k* ligaments and is not further split if:

$$\exists j_1, \ldots j_k \subset \{j_1, \ldots j_p\}\ D_{i,j_1}, \ldots D_{i,j_k} \le D. \quad (9b)$$

Otherwise **B** is on the boundary of *k* ligaments and is split (unless it reached the voxel size) and the following condition is satisfied:

$$\exists j_1, \ldots j_k \subset \{j_1, \ldots j_p\} D_{i,j_1}, \ldots D_{i,j_k} > D, d_{i,j_1}, \ldots d_{i,j_k} \le D. \quad (9c)$$

Similarly as in the previous algorithm[1], the proposed modification utilizes a first-order algebraic approximation[11,12] to determine distances $d_{i,j}$, $D_{i,j}$.

Fig. 6 illustrates the cases of the proposed algorithm for $p=2$. Note that algorithm[1] is a specific instance of the proposed algorithm for $p=1$, as it can be observed by comparison of Eq. (5a—5c) and (9a—9c).

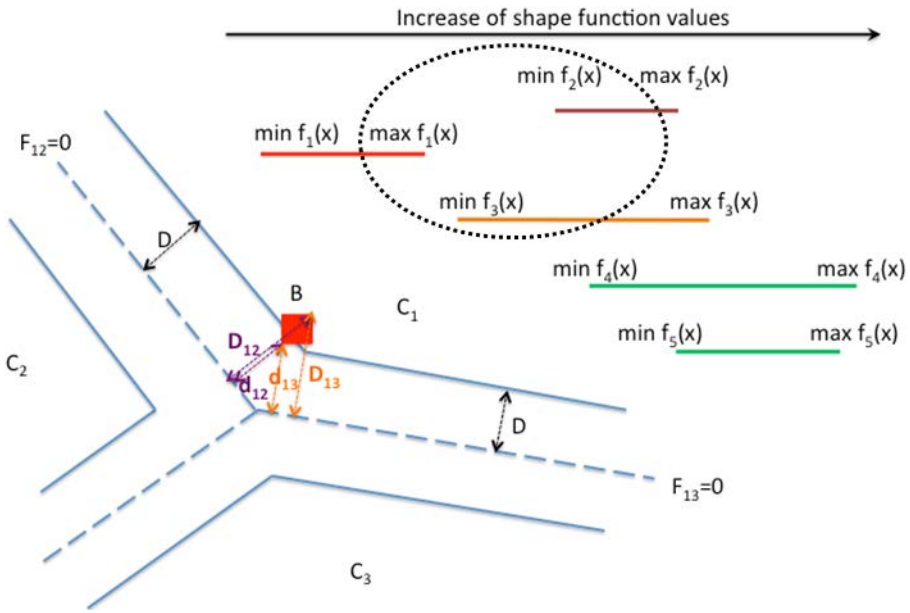

Figure 5: Illustration of the proposed algorithm (for $p=2$). The maximum of shape function f_1 within the subvolume B is smaller than the minima of other shape functions; hence the subvolume is either inside compartment 1 or on its boundary. Shape functions f_3 and f_2 have the two smallest minima larger than max $f_1(\mathbf{x})$. The algorithm determines the closest ligament to the subvolume B by calculating distances to surfaces f_1-f_3=0 and f_1-f_2=0.

Case		Property	Subvolume
Outside ligaments	1	$d_{12}>D$ $d_{13}>D$	In compartment C_1; Do not split
On ligament(s) boundary	2a	$d_{12}>D$ $d_{13}\leq D$ $D_{13}>D$	Boundary of ligament L_{13}; Split
	2b	$d_{13}>D$ $d_{12}\leq D$ $D_{12}>D$	Boundary of ligament L_{12}; Split
	3	$d_{13}\leq D$ $D_{13}>D$ $d_{12}\leq D$ $D_{12}>D$	Boundary of two ligaments L_{12}, L_{13}; Split
Inside one ligament	4a	$D_{12}\leq D$ $d_{12}>D$	In ligament L_{13}; Do not split
	4b	$D_{12}\leq D$ $d_{13}>D$	In Ligament L_{12}; Do not split
Inside one ligament, on boundary of another	5a	$D_{12}>D$ $d_{12}\leq D$ $D_{13}\leq D$	In ligament L_{13}; On ligament L_{12}; Do not split
	5b	$D_{12}>D$ $d_{13}\leq D$ $D_{12}\leq D$	In ligament L_{12}; On ligament L_{13}; Do not split
Inside two ligaments	6	$D_{12}\leq D$ $D_{13}\leq D$	In ligaments L_{12}, L_{13}; Do not split

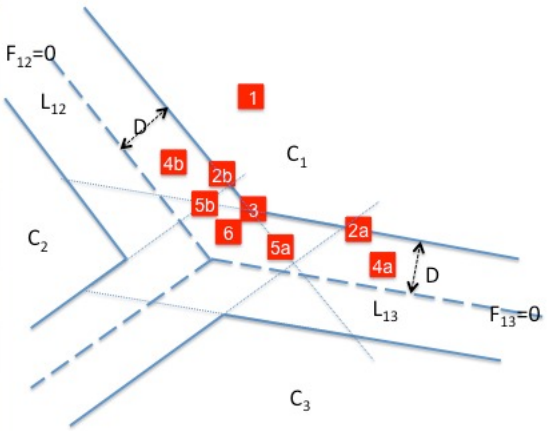

Figure 6. Different cases of the proposed algorithm (for p=2). Based on minimal and maximal distances from a subvolume to medians of two candidate ligaments, the subvolume is assigned to a compartment, to ligaments, or to their boundaries.

2.3 Evaluation of the Proposed Method

Both qualitative and quantitative evaluations of the proposed technique were performed. Phantoms were generated using the same set of parameters (i.e., nominal thickness of ligaments 2D, shape function parameters $\Sigma_i, \mathbf{s}_i, q_i, i=1,...K$ and the skin thickness), where a parameter p was varied (p=1, corresponding to the original algorithm, p=2,3). Qualitative evaluation of the proposed technique was performed by visual comparison of phantom slices and segmented ligament surfaces, and by simulating parallel X-ray projections. The proposed technique was evaluated quantitatively by counting the total number of ligament voxels, and the number of dents and corresponding voxels that were corrected using the proposed algorithm. To evaluate the improvement of smoothness of ligament boundaries, the ligaments were segmented (based on ligament labels obtained through the simulation algorithm). Subsequently, the ligament surfaces were approximated using the quadratic approximation[13]. For each voxel on the ligament surface, we calculated the distance between the voxel center and the approximating quadratic surface[14]. The accuracy of the approximation is estimated using the root mean square error (RMSE)[15]. The RMSE of corresponding ligaments in phantoms simulated using the original[1] and the proposed algorithm were compared.

3. RESULTS AND DISCUSSION

In order to perform qualitative and quantitative comparison of the old[1] and the proposed algorithm, we simulated 100μm B-cup size[16] software phantoms with K=333 compartments and selected nominal ligament thickness of 600μm (D=300μm). We compared phantoms simulated using the same set of shape functions (thus having the same structure of ligaments). All simulations were performed on iMac 3.4GHz Intel Core i7 (20GB RAM 1333MHz DDR3) under Mac OS X Lion 10.7.4 (Apple) using Matlab R2013a (Mathworks).

3.1 Qualitative Evaluation

Fig. 7 shows corresponding details from the two software phantoms. The slices contain Cooper's ligaments (blue) and adipose compartments (yellow). By comparison of figures obtained with the old and the new algorithm it is visible that the dents can be reduced or eliminated using the proposed algorithm. The reduction of the number of dents is also

visible in Fig. 8, where the surface of the ligament obtained using the proposed algorithm appears smoother than when the original algorithm is utilized.

Figure 7. A detail of a phantom simulated by old (left) and the proposed algorithm (p=2, right) indicating dent reduction.

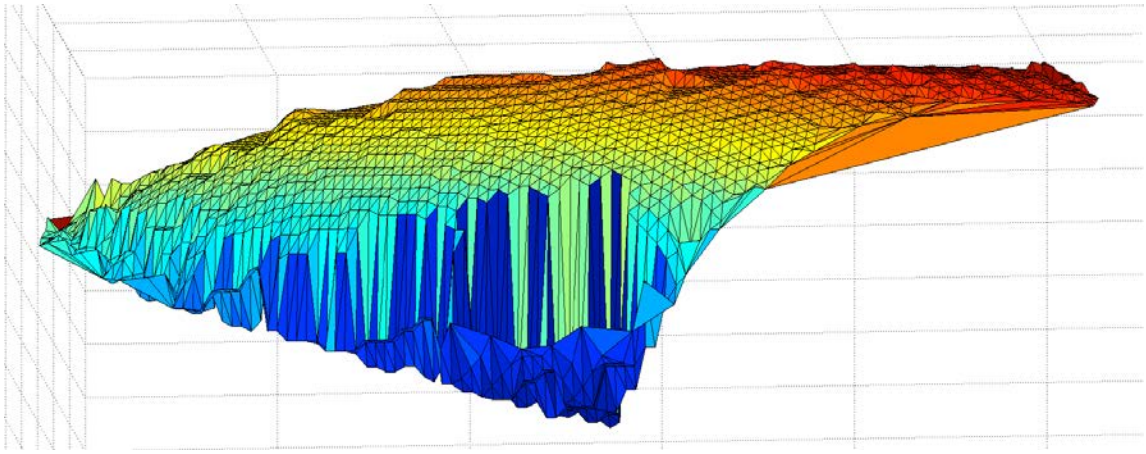

(a)

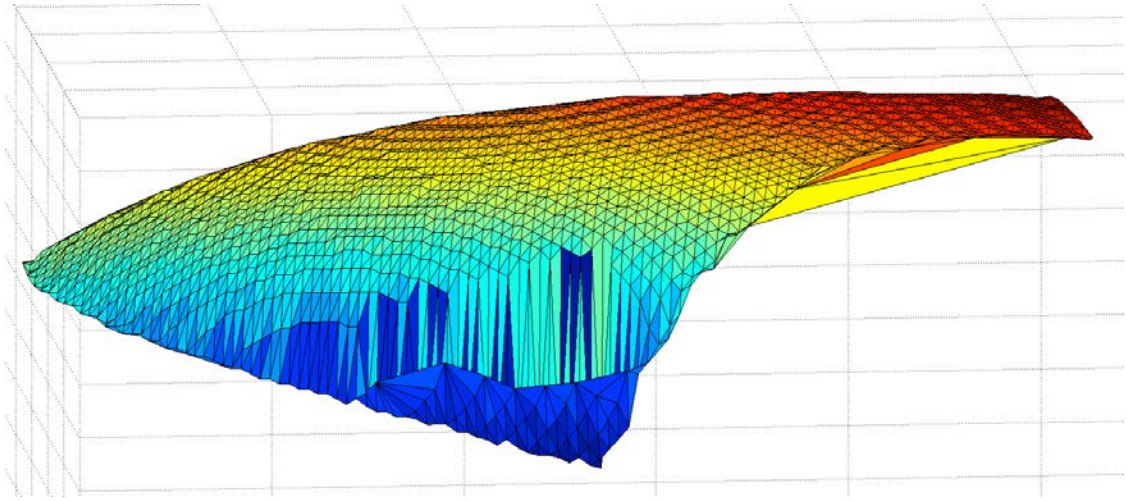

(b)

Figure 8. Three-dimensional rendering of a boundary of a segmented ligament and the root-mean-square error (RMSE) of a quadratic approximation; (a) the old algorithm[1]; RMSE=0.60 (b) the new algorithm (p=2); RMSE=0.25.

Fig. 9 shows a detail of the difference between simulated projections of the phantoms generated using the old and the new algorithm (with p=2), respectively. It can be seen that the proposed modification reduces unrealistic linear and star-like artifacts attributed to dents.

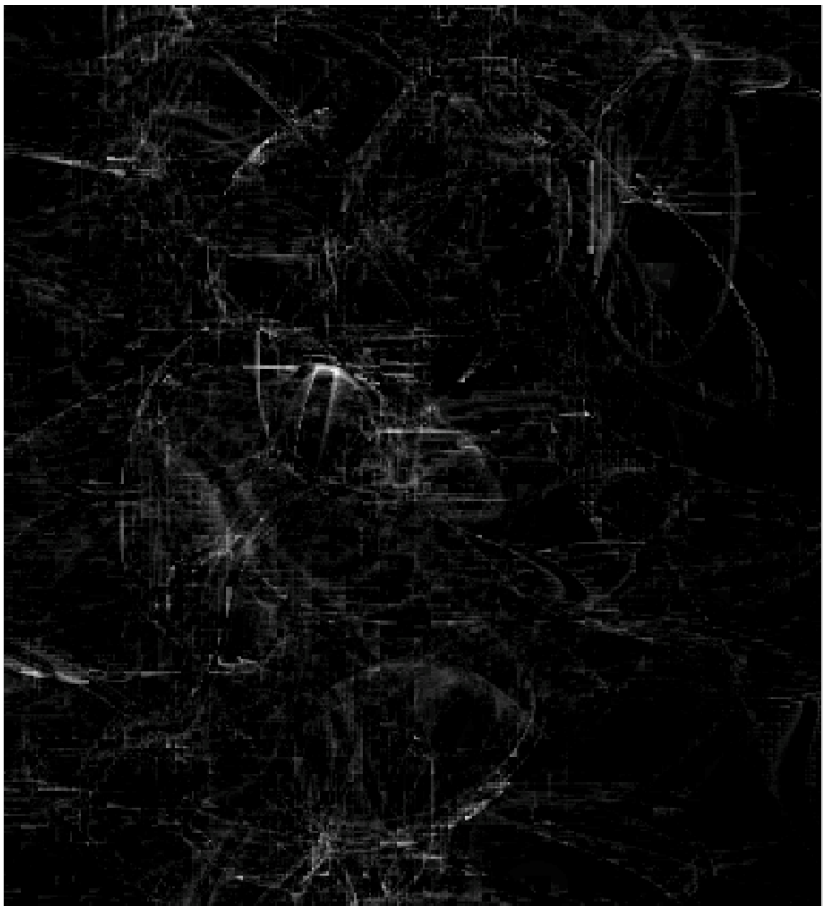

Figure 9. Difference between simulated parallel projections of phantoms simulated using the old and the proposed algorithm (p=2).

3.2 Quantitative Evaluation

Table 1 contains the comparison of the number of ligament voxels, the volume of simulated ligament tissue and elapsed time for a 100μm B-cup phantoms simulated using the old algorithm, as well as with the proposed algorithm with p=2 and p=3. As we can see, the introduction of the proposed algorithm leads to the increase of the number of the ligament voxels (and the total volume of ligaments), thus justifying our hypothesis that the proposed algorithm would reduce the number of dents. (These artifacts are replaced by ligament voxels).

This is also visible from Table 2 that shows the number of removed dents corresponding to octree nodes of different sizes. After the proposed modification, we corrected 148,105 dents, with an average size of 5.27 voxels (5.27nl). As expected, the majority of the removed dents correspond to small octree nodes, confirming the hypothesis that the dents predominantly occur at the small subvolume sizes. Further increase of the parameter p did not lead to remarkable increase of the number of ligament voxels. There was no ligament voxel in the phantom created using the old algorithm that belonged to a compartment when simulation was performed by the proposed algorithm. Hence, we empirically showed that the application of the proposed algorithm did not lead to the emergence of novel dents that did not previously exist. The formal proof of this property is part of our work in progress.

The elapsed time due to utilization of the proposed algorithm increased approximately 25% with p=2. This can be attributed to larger number of distance evaluations (when Eq. (4a) is satisfied, the new algorithm evaluates 2p

distances— $d_{i,j_1}, \ldots d_{i,j_p}$ and $D_{i,j_1}, \ldots D_{i,j_p}$ —instead of two—$d_{i,j}$ and D_i). Interestingly, with p=3, the elapsed time slightly decreased, potentially due to smaller number of affected subvolumes. The results indicate decrease in RMSE (see Fig. 8) of quadratic approximation of a ligament surface, for majority of segmented ligaments, thus suggesting the improved smoothness of the ligament surfaces. However, we observed that this approach may be hindered by numerical instability of quadratic approximation and distance computation.

Table 1. The number and volume of ligament voxels and elapsed time for B cup size phantoms with 100μm voxel size using old and the proposed algorithm, with the same set of shape functions.

Algorithm	Number of ligament voxels	Volume of ligament voxels (cm^3)	Elapsed Time
Old[1]	68,994,541	68,99	69,992s
Proposed, p=2	70,164,201	70.16	88,508s
Proposed, p=3	70,255,989	70.25	86,898s

Table 2. Number of removed dents and the corresponding number of voxels for subvolumes of different size.

Subvolume size (mm)		**3.2**	**1.6**	**0.8**	**0.4**	**0.2**
Number of	**dents**	2	107	1,378	19,921	126,697
	voxels	18	3,524	24,990	204,491	547,604

4. CONCLUSIONS

We shown that the current recursive partitioning algorithm for breast phantom generation may result in appearance of "dent" artifacts on the surfaces of simulated ligaments. Such artifacts are consequence of potential failure to properly identify a ligament closest to a phantom subvolume during the simulation process. It is demonstrated that the "dents" can result in linear and star-like artifacts in a simulated phantom projection. We proposed a novel method that reduce or eliminate "dents" and improve smoothness of ligament surfaces at the expense of increased simulation time.

Work in progress includes more comprehensive evaluation of the algorithm on a larger set of phantoms and design and implementation of objective measures of improved phantom realism. Future work includes comparison of the phantom realism achieved using the proposed algorithm and the techniques for partial volume simulation[4].

ACKNOWLEDGMENTS

This research was supported by a grant from the National Institute of General Medical Sciences (P20 GM103446) from the National Institutes of Health. Also, the work was supported in part by the US Department of Defense Breast Cancer Research Program (HBCU Partnership Training Award #BC083639), the US National Science Foundation (CREST grant #HRD-1242067), the US Department of Defense/Department of Army (Award #W911NF-11-2-0046), the US National Institutes of Health (R01 grant #CA154444), and the Komen Foundation (grant #IIR13262248).

REFERENCES

[1] Pokrajac, D.P., Maidment, A.D.A., Bakic, P.R., "Optimized generation of high resolution breast anthropomorphic software phantoms," Med. Phys. 39(4), 2290-2302 (2012).

[2] Bakic, P.R., Pokrajac, D.D., De Caro, R., Maidment, A.D.A., "Realistic simulation of breast tissue microstructure," Proc. 2014 IWDM, LNCS 8539, 348-355 (2014).

[3] Contijoch, F., Lynch, J.M., Pokrajac, D.D., Maidment, A.D.A., Bakic, P.R., "Shape analysis of simulated breast anatomical structures," Proc. SPIE 2012 8313, 83134J (2012).

[4] Chen, F., Bakic, P.R., Maidment, A.D.A., Jensen, S.T., Shi, X., Pokrajac, D.D., "Description and characterization of a novel method for partial volume simulation in software breast phantoms," IEEE Trans. Med. Imag., 34 (10), 2146-2161 (2015).

[5] Chui, J., Pokrajac, D.D., Maidment, A.D.A., Bakic, P.R., "Roadmap for efficient parallelization of breast anatomy simulation," Proc. SPIE 2012 Medical Imaging 8313, 83134T1–83134T10 (2012).
[6] Chui, J., Pokrajac, D., Maidment, A.D.A., Bakic, P.R., "Toward breast phantom simulation using GPU," Proc. IWDM, LNCS 7361, 508-515, (2012).
[7] Petkovic, M., Bakic, P.R., Maidment, A.D.A., Pokrajac, D.D., "Asymptotic number of $Z^3\Delta$ cells covering $C^{(1)}$ surface on uniform grid and complexity of recursive-partitioning simulation of septal tissue regions," Applied Mathematics and Computation 252, 264-272 (2015).
[8] Maidment A., "Virtual clinical trials for the assessment of novel breast screening modalities. Proc. 2014 IWDM LCNS 8539, 1-8 (2014).
[9] Labelle F., Shewchuk, J.R., "Anisotropic voronoi diagrams and guaranteed-quality anisotropic mesh generation," Proc. 19th annual symposium on computational geometry SCG, 191–200 (2003).
[10] Mahalanobis, P.C., "On the generalised distance in statistics," Proceedings of the National Institute of Sciences of India 2 (1), 49–55 (1936).
[11] Taubin, G., "Distance Approximations for Rasterizing Implicit Curves," ACM Trans. Graph. 13**,** 3-42 (1994).
[12] Martinez-Morera, D. Estrada Sarlabous, J., "On a distance from a point to a quadric surface," Revista Investigacion Operacional 24(2), 153-161(2003).
[13] Taubin, G., "Estimation of planar curves, surfaces, and nonplanar space curves defined by implicit equations with applications to edge and range image segmentation," IEEE Trans. PAMI 13(11), 1115-38 (2002).
[14] Schneider, P.J., Eberly, D.H. 2008, "Distance from point to a general quadratic curve or a general quadratic surface" [Online].Available: http://www.geometrictools.com/Documentation/DistancePointToQuadratic.pdf [Accessed 11/21/2013].
[15] Chai, T., Draxler, R.R., "Root mean square error (RMSE) or mean absolute error (MAE)? – Arguments against avoiding RMSE in the literature, " Geoscientific Model Development 7, 1247—1250 (2014).
[16] Bakic, P.R., Zhang, C., Maidment, A.D.A., "Development and characterization of an anthropomorphic breast software phantom based upon region-growing algorithm," Med. Phys. 38(6), 3165–3176 (2011).